

A novel class of Hsp90 inhibitors isolated by structure-based virtual screening

Hwangseo Park,^{a,†} Yun-Jung Kim^{b,†} and Ji-Sook Hahn^{b,*}

^aDepartment of Bioscience and Biotechnology, Sejong University, 98 Kunja-dong, Gwangjin-gu, Seoul 143-747, Republic of Korea

^bSchool of Chemical and Biological Engineering, Seoul National University, Sillim-dong, Gwanak-gu, Seoul 151-744, Republic of Korea

Received 12 June 2007; revised 27 August 2007; accepted 29 August 2007

Available online 1 September 2007

Abstract—A novel class of 3-phenyl-2-styryl-3H-quinazolin-4-one Hsp90 inhibitors with in vitro anti-tumor activity are identified by structure-based virtual screening of a chemical database with docking simulations in the N-terminal ATP-binding site, in vitro ATPase assay using yeast Hsp90, and cell-based Her2 degradation assay in a consecutive fashion. These results exemplify the usefulness of the structure-based virtual screening with molecular docking in drug discovery. The structural features responsible for a tight binding of the inhibitors in the active site of Hsp90 are discussed in detail.

© 2007 Elsevier Ltd. All rights reserved.

Hsp90 is one of the most abundant molecular chaperones in eukaryotic cells, playing an important role in folding, stabilization, activation, and assembly of metastable ‘client’ proteins.¹ The Hsp90 client proteins include many oncogenic signaling proteins such as Her2/ ErbB2, Akt, Raf-1, Hif-1 α , hormone receptors, survivin, mutant p53, and hTERT.^{2,3} Inhibition of Hsp90 leads to proteasome-mediated degradation of these oncogenic client proteins, placing Hsp90 as a promising new target for anti-cancer drug development.^{2,4}

The conformational change of Hsp90 derived by ATP binding and hydrolysis in the N-terminal ATPase domain is essential for the chaperone function of Hsp90.⁵ The majority of Hsp90 inhibitors developed so far inhibit Hsp90 ATPase activity by docking to the N-terminal ATP-binding pocket.⁶ This class of Hsp90 inhibitors includes natural products geldanamycin (GA) and radicicol; GA derivatives such as 17-allylamino-17-demethoxygeldanamycin (17-AAG)⁷ and 17-dimethylaminoethylamino-17-demethoxygeldanamycin (17-DMAG)⁸; purine-scaffold derivatives such as PU3, PU24FCl, and PU-H58⁹; pyrazoles¹⁰; and shepherdin, a peptidomimetic inhibitor of the survivin–Hsp90 complex.¹¹ On the

other hand, novobiocin and cisplatin have been shown to inhibit Hsp90 by binding to a potential second ATP-binding site in the C-terminus.¹² Hsp90 derived from tumor cells has especially high ATPase activity with higher binding affinity to Hsp90 inhibitors than the latent form in normal cells, allowing specific targeting of Hsp90 inhibitors to tumor cells with little inhibition of Hsp90 function in normal cells.¹³ The anti-cancer activity of Hsp90 inhibitors was validated in diverse in vitro and in vivo model systems, and 17-AAG has shown promising therapeutic outcomes in clinical trials in various types of cancer.² However, even 17-AAG has undesirable properties such as difficulty in formulation, potential toxicity, and limited water solubility, demanding for continuing development of Hsp90 inhibitors with improved pharmacological properties and efficacy.

So far, most of the Hsp90 inhibitors reported in the literature have stemmed from either the generation of the improved derivatives of pre-existing Hsp90 inhibitors or the isolation of new scaffolds by high throughput screening. The structure-based virtual screening has also been applied to the discovery of novel Hsp90 inhibitors, which leads to the identification of 1-(2-phenol)-2-naphthol¹⁴ and 5-aminoimidazole-4-carboxamide-1- β -D-ribofuranoside (AICAR)¹⁵ as new classes of Hsp90 inhibitors. In the present study, we identify a novel class of 3-phenyl-2-styryl-3H-quinazolin-4-one inhibitors of Hsp90 by means of a drug-design protocol involving a

Keywords: Hsp90 inhibitors; Cancer; 3-Phenyl-2-styryl-3H-quinazolin-4-one; Virtual screening; Drug design.

* Corresponding author. Tel.: +82 2 880 9228; fax: +82 2 888 1604; e-mail: hahnjs@snu.ac.kr

[†] These two authors are contributed equally to this work.

newly developed structure-based virtual screening tool, in vitro ATPase assay using yeast Hsp90, and cell-based Her2 degradation assay in a consecutive manner. The characteristic features that discriminate our virtual screening procedure from the others lie in the use of an accurate solvation model for putative ligands and the inclusion of crystallographic water molecules. It will be shown that the docking simulation with the improved binding free energy function can be a valuable tool for elucidating the observed activity of the identified inhibitors, as well as for enriching the chemical library used in screening assays with molecules that are likely to have biological activities.

We used the AutoDock program¹⁶ in the structure-based virtual screening of Hsp90 inhibitors because the outperformance of its scoring function over those of the others had been shown in several target proteins.¹⁷ The 3D coordinates in the crystal structure of Hsp90 in complex with a benzenesulfonamide inhibitor (PDB code: 2BZ5)¹⁴ were selected as the receptor model in the virtual screening with docking simulations. After removing the ligand and solvent molecules, hydrogen atoms were added to each protein atom. A special attention was paid to assign the protonation states of the ionizable Asp, Glu, His, and Lys residues. The side chains of Asp and Glu residues were assumed to be neutral if one of their carboxylate oxygens pointed toward a hydrogen-bond accepting group including the backbone aminocarbonyl oxygen at a distance within 3.5 Å, a generally accepted distance limit for a hydrogen bond with moderate strength.¹⁸ Similarly, the lysine side chains were protonated unless the NZ atom was in proximity of a hydrogen-bond donating group. The same procedure was applied to determine the protonation states of ND and NE atoms in His residues. Considering the significant role of the solvent-mediated interaction in protein–ligand docking,¹⁹ the structural water molecules found within 3.5 Å from the ligand in the original X-ray structure were also included in the receptor model.

The docking library of about 85,000 compounds for Hsp90 was constructed from the latest version of InterBioScreen DB (InterBioScreen Database, Moscow, <http://www.ibscreen.com>) containing approximately 30,000 natural and 290,000 synthetic compounds. This selection was based on drug-like filters that adopt only the compounds with physicochemical properties of potential drug candidates²⁰ and without reactive functional group(s). All of the compounds included in the docking library were then subjected to the Corina program to generate their 3D coordinates, followed by the assignment of Gasteiger–Marsilli atomic charges.²¹ Docking simulations with AutoDock were then carried out in the ATP-binding site of Hsp90 to score and rank the compounds in docking library according to the binding affinity for Hsp90.

In the actual docking simulation between a compound in the docking library and Hsp90, we used the empirical scoring function of the AutoDock program that has the following form:

$$\Delta G_{\text{bind}}^{\text{aq}} = W_{\text{vdW}} \sum_i \sum_{j>i} \left(\frac{A_{ij}}{r_{ij}^{12}} - \frac{B_{ij}}{r_{ij}^6} \right) + W_{\text{hbond}} \times \sum_i \sum_{j>i} E(t) \left(\frac{C_{ij}}{r_{ij}^{12}} - \frac{D_{ij}}{r_{ij}^{10}} \right) + W_{\text{elec}} \sum_i \sum_{j>i} \times \frac{q_i q_j}{\varepsilon(r_{ij}) r_{ij}} + W_{\text{tor}} N_{\text{tor}} + W_{\text{sol}} \times \sum_i^{\text{atoms}} S_i \left(O_i^{\text{max}} - \sum_{j>i}^{\text{atoms}} V_j e^{-\frac{r_{ij}^2}{2\sigma^2}} \right) \quad (1)$$

Here, W_{vdW} , W_{hbond} , W_{elec} , W_{tor} , and W_{sol} are weighting factors of van der Waals, hydrogen bond, electrostatic interactions, torsional term, and desolvation energy of inhibitors, respectively. r_{ij} represents the interatomic distance, and A_{ij} , B_{ij} , C_{ij} , and D_{ij} are related to the depths of energy well and the equilibrium separations between the two atoms. The hydrogen-bond term has an additional weighting factor, $E(t)$, representing the angle-dependent directionality. With respect to the distant-dependent dielectric constant, $\varepsilon(r_{ij})$, a sigmoidal function proposed by Mehler and Solmajer²² was used in computing the interatomic electrostatic interactions between a receptor protein and its ligands. In the entropic term, N_{tor} is the number of sp^3 bonds in the ligand. In the desolvation term, S_i and V_i are the solvation parameter and the fragmental volume of atom i ,²³ respectively, while O_i^{max} stands for the maximum atomic occupancy. In the calculation of molecular solvation free energy term in Eq. (1), we used the atomic parameters recently developed by Kang et al.²⁴ because those of the atoms other than carbon were unavailable in the current version of AutoDock. This modification of the solvation free energy term is expected to increase the accuracy in virtual screening, because the underestimation of ligand solvation often leads to the overestimation of the binding affinity of a ligand with many polar atoms.²⁵

The actual docking simulations started with the calculation of the 3D grids of interaction energy for the entire possible atom types present in chemical database. These uniquely defined potential grids for the receptor protein were then used in common for docking simulations of all compounds in docking library. As the center of the common grids, we used the center of mass coordinates of the ligand that had been removed from the ATP-binding site of Hsp90. These grid maps were of dimension $61 \times 61 \times 61$ points with the spacing of 0.375 Å, yielding a receptor model that includes atoms within 22.9 Å of the grid center. For each compound in the library, 10 docking runs were performed with the initial population of 50 individuals. Maximum number of generations and energy evaluation were set to 27,000 and 2.5×10^5 , respectively. All energy terms in Eq. (1) were calculated on the grid points with all-atom models of a protein receptor and a ligand.

Shown in Figure 1 is the overall computational and experimental strategy we have employed for the discovery of novel Hsp90 inhibitors. Of the 85,000 compounds subject to the virtual screening with docking simulation, 300 top-scored compounds were selected. Two hundred

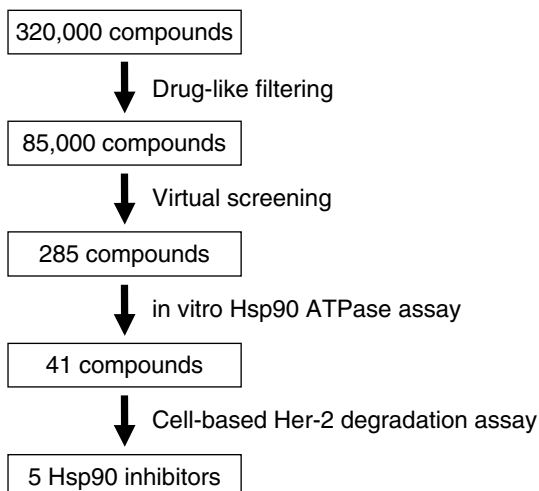


Figure 1. Integrated computational and experimental strategy for the discovery of novel Hsp90 inhibitors.

and eighty-five of them were available from the compound supplier and were tested for Hsp90 inhibitory activity by *in vitro* ATPase assay using yeast Hsp90. *Saccharomyces cerevisiae* Hsp90 protein was expressed and purified in *Escherichia coli* as a C-terminal Hig-tagged protein, and Hsp90 ATPase activity was determined in 96-well plates by colorimetric detection of the released inorganic phosphate using malachite green reagent.²⁶ We identified 41 compounds that showed more than 70% inhibition at 50 μ M concentration. This led to the discovery of several new inhibitor scaffolds with structural diversity. The scaffold structures found in more than two compounds are shown in Figure 2. These structures include previously identified pyrazole scaffold (5),¹⁰ which confirms the accuracy of the present virtual screening protocol. To the best of our knowl-

edge, however, the other seven inhibitor scaffolds have not been reported so far in the literature at least. The 3H-quinazolin-4-one scaffold was identified in five inhibitors and three of them have a common 3-phenyl-2-styryl-3H-quinazolin-4-one structure (1).

The compounds isolated from the virtual screening were tested for their effects on Her2 degradation in MCF-7 breast cancer cell line. In addition to examining the protein levels of Her2 that is one of the Hsp90 client proteins, we tested for the induction of Hsp70 to evaluate Hsp90 inhibitors. Since heat shock transcription factor (Hsf1) is negatively regulated by Hsp90, most of the Hsp90 inhibitors such as geldanamycin activate expression of Hsf1 target genes including HSP70.²⁷ MCF-7 cells were treated with 30 μ M of each compound for 24 h, and the expression levels of Her2 and Hsp70 were detected by Western blotting analysis. We identified five compounds which conferred more than 50% reduction in Her2 protein levels compared to the vehicle control while inducing Hsp70 expression. Other compounds might have a limited accessibility to Hsp90 *in vivo*. Three out of the five isolated compounds share a common 3-phenyl-2-styryl-3H-quinazolin-4-one scaffold as shown in Figure 3. All three compounds showed similar potency toward Her2 degradation with reduced efficiency compared to geldanamycin (Fig. 4). The newly identified compounds inhibited Hsp90 ATPase activity with IC₅₀ values from 20.0 to 31.8 μ M. Geldanamycin gave an IC₅₀ of 2.3 μ M in our assay system (Table 1). The antiproliferation activities of the Hsp90 inhibitors were measured by sulforhodamine B (SRB) assay²⁸ after 4 day exposure of the compounds. The 3-phenyl-2-styryl-3H-quinazolin-4-one compounds effectively inhibited growth of MCF-7 cells with GI₅₀ of around 25.4–35.6 μ M, which are only 2.6- to 3.7-fold higher than GI₅₀ for geldanamycin (9.6 μ M) (Table 1).

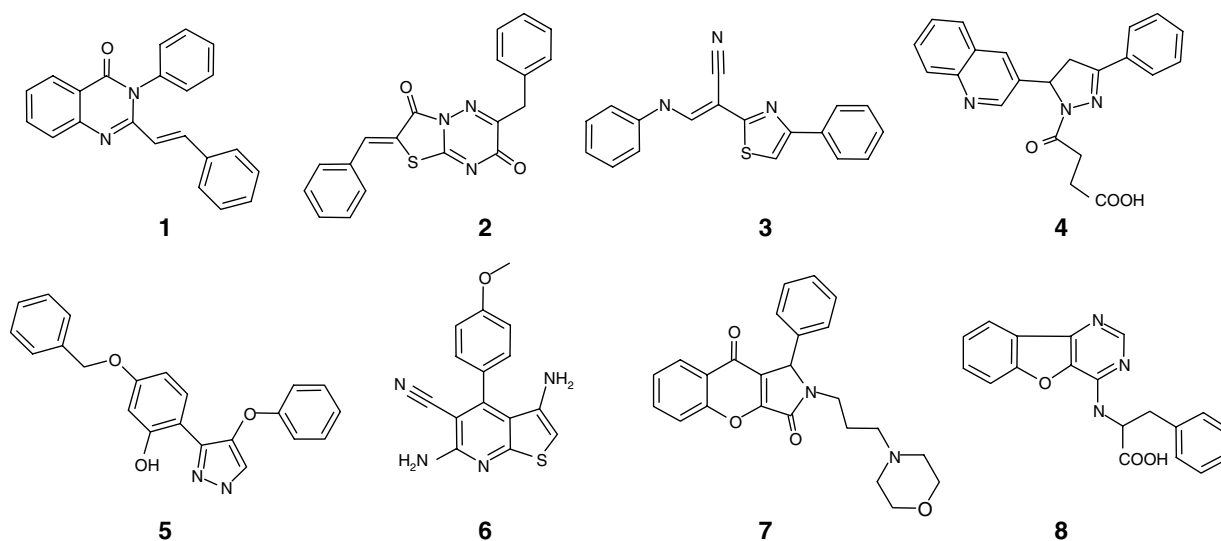


Figure 2. Chemical structures of the newly identified Hsp90 inhibitor scaffolds. The IUPAC names for the compounds are: (1) 3-phenyl-2-styryl-3H-quinazolin-4-one, (2) 6-benzyl-2-benzylidene-thiazolo[3,2-b][1,2,4]triazine-3,7-dione, (3) 3-phenylamino-2-(4-phenylthiazol-2-yl)acrylonitrile, (4) 4-oxo-4-(3-phenyl-5-quinolin-3-yl-4,5-dihydropyrazol-1-yl)butyric acid, (5) 5-benzoyloxy-2-(4-phenoxy-1H-pyrazol-3-yl)phenol, (6) 3,6-diamino-4-(4-methoxyphenyl)-thieno[2,3-b]pyridine-5-carbonitrile, (7) 2-(3-morpholin-4-yl-propyl)-1-phenyl-1,2-dihydro-4-oxa-2-aza-cyclopenta[b]naphthalene-3,9-dione, and (8) 2-(benzo[4,5]furo[3,2-d]pyrimidin-4-ylamino)-3-phenylpropionic acid.

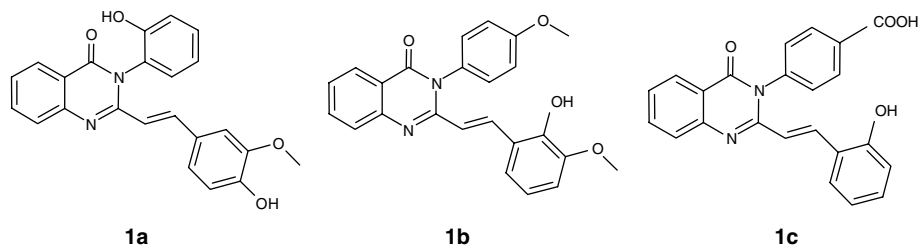


Figure 3. Chemical structures of the three 3-phenyl-2-styryl-3H-quinazolin-4-one inhibitors exhibiting Her2 degradation in cell-based assay. The IUPAC names for **1a**, **1b**, and **1c** are 2-[2-(4-hydroxy-3-methoxyphenyl)ethenyl]-3-(2-hydroxyphenyl)-3H-quinazolin-4-one, 2-[2-(2-hydroxy-3-methoxyphenyl)ethenyl]-3-(4-methoxyphenyl)-3H-quinazolin-4-one, and 4-{2-[2-(2-hydroxyphenyl)ethenyl]-4-oxo-4H-quinazolin-3-yl}benzoic acid, respectively.

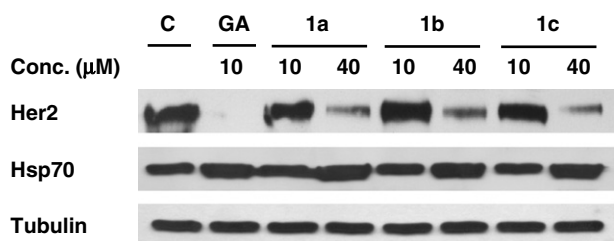


Figure 4. Effects of Hsp90 inhibitors on Her2 degradation and Hsp70 induction. MCF-7 cells were treated for 24 h with indicated concentrations of geldanamycin (GA) or three 3-phenyl-2-styryl-3H-quinazolin-4-one compounds dissolved in 0.4% DMSO or 0.4% DMSO (C) for control. The expression levels of Her2 and Hsp70 were detected by Western blotting analysis. Tubulin was used as a loading control.

We analyzed the interactions between Hsp90 inhibitors and Hsp90 by molecular modeling. Table 2 lists the calculated binding free energies of the three identified Hsp90 inhibitors. Keeping it in mind that the binding free energy of a protein–ligand complex in solution (ΔG_b^{sol}) can be approximated as the difference between that in the gas phase (ΔG_b^{gas}) and the solvation free energy of the ligand (ΔG^{sol}),²⁵ we computed the two energy components separately to estimate their relative contributions to ΔG_b^{sol} . We note that ΔG_b^{gas} becomes more favorable with the introduction of the carboxyl group at the side chain of the 3-phenyl-2-styryl-3H-quinazo-

lin-4-one scaffold (**1c**). Simultaneously, however, the solvation free energy becomes more negative, which indicates an increase in the desolvation cost for the complexation of **1c** in the ATP-binding site of Hsp90. As a result, no significant difference in ΔG_b^{sol} was found among the three identified Hsp90 inhibitors. These results indicate that the increased stabilization in solution due to structural changes should be overcome by an even stronger enzyme–inhibitor interaction in order to enhance the inhibitory activity.

To obtain some energetic and structural insight into the inhibitory mechanisms by the three identified inhibitors for Hsp90, their binding modes in the ATP-binding site of Hsp90 were calculated using AutoDock program with the procedure described in the experimental section. The calculated binding modes of the three inhibitors are compared in Figure 5. It is noted that consistent with the similarity in inhibitory activity, all of the three Hsp90 inhibitors fit the binding pocket in a similar fashion. In all three cases, the N-3 atom on the inhibitor quinazolin ring forms a hydrogen bond with the side-chain amide group of Asn51. The inhibitors can be further

Table 1. Inhibitory effects of 3-phenyl-2-styryl-3H-quinazolin-4-one compounds on yeast Hsp90 ATPase and proliferation of MCF-7 human breast cancer cell line

Compound	Geldanamycin	1a	1b	1c
IC ₅₀ (μM) ^a	2.3	31.8	20.0	22.0
GI ₅₀ (μM) ^a	9.6	25.4	27.5	35.6

IC₅₀, the concentration inhibiting Hsp90 ATPase activity by 50%.

GI₅₀, the concentration inhibiting cell growth by 50%.

^a Values correspond to $n = 2$.

Table 2. Calculated binding free energy in the gas phase, solvation free energy, and binding free energy in solution for the three Hsp90 inhibitors

Compound	ΔG_b^{gas}	ΔG^{sol}	ΔG_b^{sol}
1a	−29.09	−6.51	−22.58
1b	−29.12	−6.36	−22.76
1c	−30.63	−8.01	−22.62

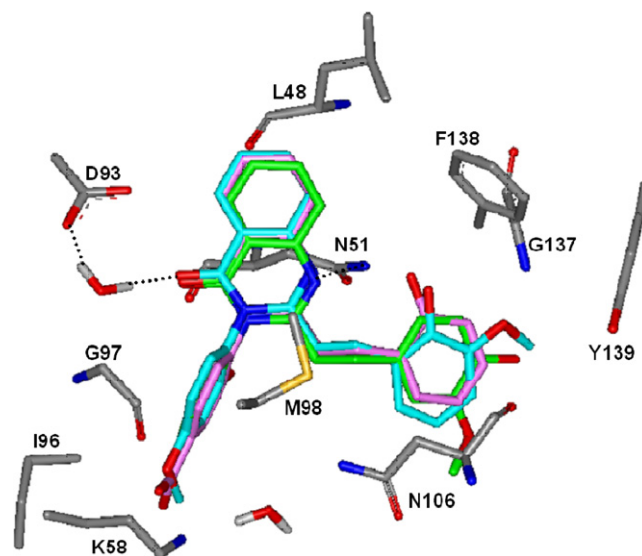


Figure 5. Comparative view of the calculated binding modes of three inhibitors in the ATP-binding site of Hsp90. Carbon atoms of **1a**, **1b**, and **1c** are indicated in green, cyan, and pink, respectively. All hydrogen atoms but those of the structural water molecules are omitted for visual clarity. Each dotted line indicates a hydrogen bond.

stabilized in the ATP-binding site by the establishment of an additional hydrogen bond between the carbonyl oxygen and one of the structural water molecules that is in turn hydrogen bonded to the side-chain carboxylic acid group of Asp93. This exemplifies the involvement of a solvent-mediated hydrogen bond, which has been considered as one of the significant binding forces in protein–ligand interactions in aqueous solution,¹⁹ in the stabilization of the inhibitors in the ATP-binding site of Hsp90. Judging from the fact that the O–H···O hydrogen bond is stronger than the N–H···N one,¹⁸ such a solvent-mediated hydrogen bond is likely to play an essential role in the inhibition of Hsp90 by the 3-phenyl-2-styryl-3H-quinazolin-4-one inhibitors. This is believed to serve as key information for future designing of new potent Hsp90 inhibitors.

In conclusion, by virtue of the structure-based virtual screening under consideration of the effects of ligand solvation and structural water molecules, we have been able to identify 41 novel Hsp90 inhibitors with low micromolar Hsp90 ATPase inhibitory activity. The subsequent cell-based Her2 degradation assay led to the identification of three 3-phenyl-2-styryl-3H-quinazolin-4-one inhibitors exhibiting antiproliferation activity against MCF-7 breast cancer cell line. Docking simulation of these inhibitors in the ATP-binding site of Hsp90 showed that a direct hydrogen bond with the side chain of Asn51 and a solvent-mediated hydrogen bond with the side chain of Asp93 should be significant binding forces to stabilize the enzyme–inhibitor complexes. These results exemplify the importance of the role of structural water molecules in Hsp90–ligand interactions. The present study demonstrates the usefulness of the automated AutoDock program with the improved scoring function as a docking program for virtual screening as well as for binding mode analysis to elucidate the activities of identified inhibitors. The novel 3-phenyl-2-styryl-3H-quinazolin-4-one inhibitors of Hsp90 identified in this study are expected to find their ways as a new starting point to develop more potent anti-cancer drugs.

Acknowledgments

This work was supported by grants from Korea Research Foundation (2005-005-J16002) and the Basic Research Program of the Korea Science & Engineering Foundation (R01-2006-000-10255-0).

References and notes

- Csermely, P.; Schnaider, T.; Soti, C.; Prohaszka, Z.; Nardai, G. *Pharmacol. Ther.* **1998**, *79*, 129; Richter, K.; Buchner, J. *J. Cell Physiol.* **2001**, *188*, 281.
- Sharp, S.; Workman, P. *Adv. Cancer Res.* **2006**, *95*, 323.
- Neckers, L.; Ivy, S. P. *Curr. Opin. Oncol.* **2003**, *15*, 419; Fortugno, P.; Beltrami, E.; Plescia, J.; Fontana, J.; Pradhan, D.; Marchisio, P. C.; Sessa, W. C.; Altieri, D. C. *Proc. Natl. Acad. Sci. U.S.A.* **2003**, *100*, 13791.
- Calderwood, S. K.; Khaleque, M. A.; Sawyer, D. B.; Ciocca, D. R. *Trends Biochem. Sci.* **2006**, *31*, 164; Chiosis, G.; Vilenchik, M.; Kim, J.; Solit, D. *Drug Discovery Today* **2004**, *9*, 881.
- Pearl, L. H.; Prodromou, C. *Annu. Rev. Biochem.* **2006**, *75*, 271.
- Stebbins, C. E.; Russo, A. A.; Schneider, C.; Rosen, N.; Hartl, F. U.; Pavletich, N. P. *Cell* **1997**, *89*, 239; Roe, S. M.; Prodromou, C.; O'Brien, R.; Ladbury, J. E.; Piper, P. W.; Pearl, L. H. *J. Med. Chem.* **1999**, *42*, 260.
- Schulte, T. W.; Neckers, L. M. *Cancer Chemother. Pharmacol.* **1998**, *42*, 273.
- Egorin, M. J.; Lagattuta, T. F.; Hamburger, D. R.; Covey, J. M.; White, K. D.; Musser, S. M.; Eiseman, J. L. *Cancer Chemother. Pharmacol.* **2002**, *49*, 7.
- Chiosis, G.; Lucas, B.; Shtil, A.; Huezo, H.; Rosen, N. *Bioorg. Med. Chem.* **2002**, *10*, 3555; He, H.; Zatorska, D.; Kim, J.; Aguirre, J.; Llauger, L.; She, Y.; Wu, N.; Immormino, R. M.; Gewirth, D. T.; Chiosis, G. *J. Med. Chem.* **2006**, *49*, 381.
- Cheung, K. M.; Matthews, T. P.; James, K.; Rowlands, M. G.; Boxall, K. J.; Sharp, S. Y.; Maloney, A.; Roe, S. M.; Prodromou, C.; Pearl, L. H.; Aherne, G. W.; McDonald, E.; Workman, P. *Bioorg. Med. Chem. Lett.* **2005**, *15*, 3338; McDonald, E.; Jones, K.; Brough, P. A.; Drysdale, M. J.; Workman, P. *Curr. Top. Med. Chem.* **2006**, *6*, 1193.
- Plescia, J.; Salz, W.; Xia, F.; Pennati, M.; Zaffaroni, N.; Daidone, M. G.; Meli, M.; Dohi, T.; Fortugno, P.; Nefedova, Y.; Gabrilovich, D. I.; Colombo, G.; Altieri, D. C. *Cancer Cell* **2005**, *7*, 457.
- Marcu, M. G.; Chadli, A.; Bouhouche, I.; Catelli, M.; Neckers, L. M. *J. Biol. Chem.* **2000**, *275*, 37181; Soti, C.; Racz, A.; Csermely, P. *J. Biol. Chem.* **2002**, *277*, 7066.
- Kamal, A.; Thao, L.; Sensintaffar, J.; Zhang, L.; Boehm, M. F.; Fritz, L. C.; Burrows, F. J. *Nature* **2003**, *425*, 407.
- Barril, X.; Brough, P.; Drysdale, M.; Hubbard, R. E.; Massey, A.; Surgenor, A.; Wright, L. *Bioorg. Med. Chem. Lett.* **2005**, *15*, 5187.
- Meli, M.; Pennati, M.; Curto, M.; Daidone, M. G.; Plescia, J.; Toba, S.; Altieri, D. C.; Zaffaroni, N.; Colombo, G. *J. Med. Chem.* **2006**, *49*, 7721.
- Morris, G. M.; Goodsell, D. S.; Halliday, R. S.; Huey, R.; Hart, W. E.; Belew, R. K.; Olson, A. J. *J. Comput. Chem.* **1998**, *19*, 1639.
- Park, H.; Lee, J.; Lee, S. *Proteins* **2006**, *65*, 549.
- Jeffrey, G. A. *An Introduction to Hydrogen bonding*; Oxford University Press: Oxford, 1997.
- Verdonk, M. L.; Chessari, G.; Cole, J. C.; Hartshorn, M. J.; Murray, C. W.; Nissink, J. W.; Taylor, R. D.; Taylor, R. *J. Med. Chem.* **2005**, *48*, 6504.
- Lipinski, C. A.; Lombardo, F.; Dominy, B. W.; Feeney, P. *J. Adv. Drug Delivery Rev.* **1997**, *23*, 3.
- Gasteiger, J.; Marsilli, M. *Tetrahedron* **1980**, *36*, 3219.
- Mehler, E. L.; Solmajer, T. *Protein Eng.* **1991**, *4*, 903.
- Stouten, P. F. W.; Frömmel, C.; Nakamura, H.; Sander, C. *Mol. Simul.* **1993**, *10*, 97.
- Kang, H.; Choi, H.; Park, H. *J. Chem. Inf. Model* **2007**, *47*, 509.
- Shoichet, B. K.; Leach, A. R.; Kuntz, I. D. *Proteins* **1999**, *34*, 4.
- Rowlands, M. G.; Newbatt, Y. M.; Prodromou, C.; Pearl, L. H.; Workman, P.; Aherne, W. *Anal. Biochem.* **2004**, *327*, 176.
- Zou, J.; Guo, Y.; Guettouche, T.; Smith, D. F.; Voellmy, R. *Cell* **1998**, *94*, 471.
- Skehan, P.; Storeng, R.; Scudiero, D.; Monks, A.; McMahon, J.; Vistica, D.; Warren, J. T.; Bokesch, H.; Kenney, S.; Boyd, M. R. *J. Natl. Cancer Inst.* **1990**, *82*, 1107.